A GIS Open-Data Co-Simulation Platform for Photovoltaic Integration in Residential Urban Areas

Engineering 26 (2023) 198–213

Contents lists available at ScienceDirect

Engineering

journal homepage: www.elsevier.com/locate/eng

Research
Energy Systems Engineering—Article

A GIS Open-Data Co-Simulation Platform for Photovoltaic Integration in Residential Urban Areas

Marco Massano [a,*], Enrico Macii [a], Andrea Lanzini [b], Edoardo Patti [c], Lorenzo Bottaccioli [a,*]

[a] Interuniversity Department of Regional and Urban Studies and Planning, Politecnico di Torino, Torino 10129, Italy
[b] Department of Energy "Galileo Ferraris", Politecnico di Torino, Torino 10129, Italy
[c] Department of Control and Computer Engineering, Politecnico di Torino, Torino 10129, Italy

ARTICLE INFO

Article history:
Received 12 January 2022
Revised 19 June 2022
Accepted 28 June 2022
Available online 27 August 2022

Keywords:
Energy informatics
Geographic information system
Load estimation
Open data
Photovoltaic
Residential
Urban planning
Co-simulation

ABSTRACT

The rising awareness of environmental issues and the increase of renewable energy sources (RESs) has led to a shift in energy production toward RES, such as photovoltaic (PV) systems, and toward a distributed generation (DG) model of energy production that requires systems in which energy is generated, stored, and consumed locally. In this work, we present a methodology that integrates geographic information system (GIS)-based PV potential assessment procedures with models for the estimation of both energy generation and consumption profiles. In particular, we have created an innovative infrastructure that co-simulates PV integration on building rooftops together with an analysis of households' electricity demand. Our model relies on high spatiotemporal resolution and considers both shadowing effects and real-sky conditions for solar radiation estimation. It integrates methodologies to estimate energy demand with a high temporal resolution, accounting for realistic populations with realistic consumption profiles. Such a solution enables concrete recommendations to be drawn in order to promote an understanding of urban energy systems and the integration of RES in the context of future smart cities. The proposed methodology is tested and validated within the municipality of Turin, Italy. For the whole municipality, we estimate both the electricity absorbed from the residential sector (simulating a realistic population) and the electrical energy that could be produced by installing PV systems on buildings' rooftops (considering two different scenarios, with the former using only the rooftops of residential buildings and the latter using all available rooftops). The capabilities of the platform are explored through an in-depth analysis of the obtained results. Generated power and energy profiles are presented, emphasizing the flexibility of the resolution of the spatial and temporal results. Additional energy indicators are presented for the self-consumption of produced energy and the avoidance of CO_2 emissions.

1. Introduction

One of the main challenges of our century, as highlighted by the European Commission, among others, is to reduce greenhouse gas emissions [1]. Many countries are investing in the development and deployment of renewable energy source (RES) systems in order to reduce their dependence on fossil fuels for energy generation. This aim implies both an increasing installation of RES and the smart use of energy in our cities. Indeed, the increase in renewable energy production is changing how we produce and manage energy. Green energy sources are irregular by nature, as they depend on environmental features that typically change over time and space. As a result, we are transitioning from a unified and centralized energy production method to a more flexible and distributed one. Successfully shifting toward a distributed generation (DG) model of energy production is becoming increasingly important, and requires a production system in which energy is generated, stored, and consumed locally.

This decentralization trend empowers consumers, who are encouraged to generate their own electricity and consequently reduce their energy demand from the grid. In addition to the self-consumption of locally produced electricity within individual households, more advanced concepts such as renewable energy communities (RECs) have been developed. An REC is a microsystem that can self-produce renewable energy or invest in its production, thereby covering its own energy needs [2]. In June

* Corresponding authors.
E-mail addresses: marco.massano@polito.it (M. Massano), lorenzo.bottaccioli@polito.it (L. Bottaccioli).

https://doi.org/10.1016/j.eng.2022.06.020

2018, the European Union agreed on a corresponding legal framework as part of a recast of the Renewable Energy Directive (a.k.a. RED II) [3], which took effect in December 2018. When consumers acquire ownership of renewable energies, they can become prosumers, generating part of the energy they consume [4,5]. Consumer (co)ownership in renewable energy is an essential cornerstone to the overall success of the energy transition. These new challenges for the energy sector call for solutions that allow the optimization of energy flows by connecting decentralized energy suppliers with consumers. Structuring an REC involves many resources and accomplishments, from the legal and the economic frameworks through which RECs can subsist, to technical and engineering architecture for the operation and maintenance of the community.

The integration of DG resources changes the balance of the actual electricity distribution network by shifting both the time of energy generation and the location of production. The novel concept of the smart grid promotes novel services for the smart management of energy loads and energy production. To develop and test such new services, we need massive and pervasive information about the status of the grid, at even the household and appliance level. In the near future, information and communication technologies (ICT)—especially advanced metering infrastructure (AMI)—will allow pervasive data retrieval and collection of a large amount of energy-related information on the consumption behaviors of citizens [6,7]. However, the presence of AMI is still limited, although it is growing. Regarding residential energy consumption profiles in particular, there is still a lack of distributed sensors capable of collecting and exchanging energy-related data. To overcome the lack of actual information, we need realistic models to produce realistic simulated synthetic data. The challenge considered in this research is the capability to simulate all the different entities in an REC, from generation to consumption.

In the development of simulation and modeling tools for distributed energy systems, geographic information systems (GIS) play a crucial role. According to the Environmental System Research Institute, GIS are "an organized collection of computer hardware, software, geographic data, and personnel designed to efficiently capture, store, update, manipulate, analyze, and display all forms of geographically referenced information" [8]. GIS provide the geographical basis for simulating and modeling smart urban energy systems (UESs) [9]. In particular, GIS provide heterogeneous information on the environment of the area of interest, such as information on population distribution, buildings' locations and characteristics, local energy resources, or the localization of sensors. Furthermore, GIS make it possible to perform accurate simulations in a region for planning and evaluating the power production from renewable and distributed energy sources. Finally, GIS make it possible to build thematic maps, which are essential for presenting and visualizing results for planners and decision-makers. Another key aspect is the importance of working with open geospatial data, which can be freely downloaded, visualized, and shared.

In this paper, we review GIS-based spatial and spatiotemporal models and methods for modeling UES and thereby demonstrate that methodologies to estimate both photovoltaic (PV) potentials and energy demand in high spatiotemporal resolution are still missing. We present a methodology that integrates GIS-based PV potential assessment procedures with models to estimate both energy generation and energy consumption profiles in high spatiotemporal resolution. Our methodology is based on open-source GIS solutions and can model urban electricity generation and consumption, starting from publicly available data. Furthermore, we integrate a technique to simulate realistic synthetic populations, thus generating an additional open dataset. We have created an innovative co-simulation infrastructure, which builds on a modular framework to perform co-simulation with different energy scenarios. In particular, this work assesses the integration of PVs on building rooftops with an analysis of households' electricity demand. Within this research work, we test the methodology in a real urban context, applying it to the city of Turin, Italy. By providing the requested input information, the co-simulation infrastructure can be easily replicated in other realities, such as city districts, rural areas, or entire cities. From a spatial point of view, the proposed methodology can generate results ranging from a single building rooftop to a whole region. From a temporal point of view, it can reproduce power and energy profiles extending from 10 min to daily or yearly resolution. The high spatiotemporal discretization employed by the proposed methodology enables us to make accurate estimations of both energy profiles and environmental indicators.

The rest of this work is organized as follows. Section 2 reviews relevant state-of-the-art solutions for modeling and simulating UES. Section 3 introduces the proposed methodology and the design of the co-simulation infrastructure. Section 4 presents the experimental results obtained by applying the proposed methodology in a real-world city. Section 5 presents the current limitations of the proposed co-simulation infrastructure and future works. Finally, Section 6 provides concluding remarks.

2. Related work

To identify GIS-based methodologies for the estimation of RES potentials and the determination of energy demand, we conducted a comprehensive literature review. A wide range of methodologies have been developed to integrate PV systems in urban environments, and these have been applied to different study areas and spatiotemporal resolutions. For all the reviewed solutions, we paid particular attention to the granularity of both spatial and temporal resolution, enhancing those methodologies that favor higher discretization. During the revision process, special attention was given to the nature of the tools and data sources employed (i.e., proprietary or open) and to the technical structure of the methodologies (examples of the main keywords used include modularity, flexibility, and co-simulation). The solutions in the literature are specially designed to estimate only the generation side of the UES. Therefore, in the introductive Section 2.1, we analyze the main expertise required to determine and integrate PV power production. We present methodologies in the literature from solutions at the country scale (Section 2.2) and at the urban scale (Section 2.3) to solutions with a high resolution (Section 2.4). We then analyze those solutions that combine both the production and the demand side of PV systems integration (Section 2.5). The last analyzed category includes solutions that are developed as a full-service platform (Section 2.6). Finally, in Section 2.7, we highlight the main limitations and gaps in this field and present the scientific contributions of our work. The results of the literature review are summarized in Table 1, which reports all the significant features outlined in this review, highlighting the main technical characteristics that distinguish each methodology [10–31].

2.1. Potential PV elements

To assess the potential of rooftop-mounted PV systems, the main elements to be determined are the effective suitable rooftop area and the real solar irradiance that impinges on the surface. A high spatial resolution makes it possible to retrieve rooftop properties such as altitude, slope (or inclination), and aspect (or orientation). Given these parameters, it is possible to determine the portion of the roof that is suitable for the installation of PV systems, excluding objects such as dormers and chimneys. To this end, two kinds of data models are predominantly used: digital

Table 1
Overview of urban energy system GIS-based spatiotemporal methodologies.

Refs.	Main context	Min spatial resolution	Multiscale spatial resolution	Shadows	Min temporal resolution	Multiscale temporal resolution	Real-sky	Loads	Synth-pop	Open dataset	Co-sim
This work	—	25 cm	√	√	10 min	√	√	√	√	√	√
Suri et al. [10]	Country scale (Section 2.2)	1 km	√	×	1 month	√	×	×	×	×	×
HOMER [11]	Country scale (Section 2.2)	N.A.	√	×	1 month	√	×	√	×	×	×
Lund et al. [12]	Country scale (Section 2.2)	N.A.	√	×	1 h	√	×	√	×	×	×
Wiginton et al. [13]	Urban scale (Section 2.3)	20 cm	×	√	1 year	×	×	×	×	√	×
Bergamasco and Asinari [14,15]	Urban scale (Section 2.3)	N.A.	×	×	1 year	×	×	×	×	√	×
Mainzer et al. [16]	Urban scale (Section 2.3)	N.A.	N.A.	×	15 min	×	×	×	×	√	×
Assouline et al. [17]	Urban scale (Section 2.3)	2 m	√	×	1 month	N.A.	×	×	×	√	×
Kodysh et al. [18]	High spatial resolution (Section 2.4)	1 m	√	√	1 year	√	×	×	×	√	×
Hofierka and Kaňuk [19]	High spatial resolution (Section 2.4)	1 m	×	√	1 year	√	√	×	×	√	×
Brito et al. [20]	High spatial resolution (Section 2.4)	1 m	×	×	1 year	×	×	×	×	√	×
Nguyen and Pearce [21]	High spatial resolution (Section 2.4)	55 cm	√	√	3 min	√	×	×	×	√	×
Agugiaro et al. [22]	High spatial resolution (Section 2.4)	1 m	×	√	1 year	√	√	×	×	√	×
Bottaccioli et al. [23]	High spatial resolution (Section 2.4)	25 cm	√	√	15 min	√	√	×	×	√	×
Litjens et al. [24]	Electricity demand integration (Section 2.5)	50 cm	√	√	1 month	√	×	√	×	×	×
Ramirez Camargo et al. [25]	Electricity demand integration (Section 2.5)	1 m	√	√	sub-hourly	√	√	√	×	√	×
Groppi et al. [26]	Electricity demand integration (Section 2.5)	N.A.	N.A.	×	1 year	×	×	√	×	×	×
Luthander et al. [27]	Electricity demand integration (Section 2.5)	50 cm	×	×	1 year	×	×	√	×	×	×
Girardin et al. [28]	Full-service platforms (Section 2.6)	N.A.	√	×	1 year	√	×	√	×	√	×
Berkeley Lab [29]	Full-service platforms (Section 2.6)	N.A.	√	×	1 h	√	×	√	×	×	×
Alhamwi et al. [30]	Full-service platforms (Section 2.6)	N.A.	√	×	15 min	√	×	√	×	√	×
Fonseca et al. [31]	Full-service platforms (Section 2.6)	2 m	√	×	1 h	√	×	√	×	√	×

Min: minimum; Co-sim: co-simulation; Synth-pop: synthetic populations; N.A.: not available; √: presence; ×: lack.

orthophotos (DOPs) and digital surface models (DSMs). DOPs are aerial photography or satellite imagery that has been geometrically corrected (orthorectified). When combined with image classification and object-recognition techniques, DOPs can be used to retrieve building characteristics, reaching spatial resolutions on the order of a few meters. A DSM is a digital model of terrain surface created from elevation data. The main techniques to generate DSMs are light detection and ranging (LiDAR; i.e., laser scanning) and photogrammetric point clouds. A DSM represents the earth's surface and includes all the objects on it (e.g., trees and buildings). DSMs can reach a very high spatial resolution of just a few centimeters. For this reason, DSMs are mostly used to shape building footprints. DSMs also enable the estimation of shadowing effects of near and distant objects, which is difficult to achieve with DOPs. Ruiz-Arias et al. [32], Haurant et al. [33], and Ramirez Camargo and Dorner [34] demonstrated that significant improvements can be achieved in estimating solar resources when the resolution of satellite images is increased and shadowing is considered using high-resolution DSMs.

Many tools have been developed to compute the real solar irradiance that impinges on a surface, such as Solar Analyst and r.sun. Solar Analyst is provided by ArcGIS [35], a proprietary software, while r.sun is part of the open-source GRASS-GIS platform [19]. Both have been used to develop a large number of cadastres for solar irradiance all around the globe. These cadastres enable the calculation of theoretical solar radiation potential based on geographic parameters (i.e., latitude and longitude). This theoretical calculation corresponds to the solar radiation under clear-sky conditions. The calculation of solar radiation under real-sky conditions integrates real meteorological data, which considers clouds and real weather conditions.

2.2. Country scale

Studies on a country scale have been published with a spatial resolution ranging from several kilometers to a dozen meters. Suri et al. [10] pioneered the use of GIS in this context by combining r.sun with measurements from 566 ground meteorological stations to generate a database of yearly and monthly solar radiation maps with a spatial resolution of 1 km in Europe. The resulting PV potential database was made available through the PV-GIS platform [36]. PVWATTS [37], i-GUESS [38], HOMER [11], and EnergyPLAN [12] are web applications for regional energy planning to estimate yearly, monthly, and hourly PV production using a typical meteorological year (TMY). They provide maps for yearly solar radiation and PV potential, and support the design of microgrid systems by evaluating different configurations based on their life-cycle cost. The main limitation of these solutions lies in their coarse resolution, both spatial (1 km) and temporal (1 month), which does not enable accurate calculations for PV energy production. Furthermore, none of these solutions considers real-sky conditions. Finally, most of these solar radiation maps are proprietary, and a final user can make calculations only by using the proposed web-based solution.

2.3. Urban scale

At the urban scale, the spatial resolution can drop to below 1 m. One solution is to combine high-resolution DOPs with image classification and object-recognition methodologies. Wiginton et al. [13] used both building footprint vector data and a feature analyst extraction software on DOPs with a 20 cm resolution to identify potential rooftop areas suitable for PV deployment in southeast Ontario, Canada. These areas were reduced by including factors such as shading and orientation. The PV energy output was calculated for different technologies, considering the yearly cumulated average solar radiation for every municipality under analysis as the driving factor. Bergamasco and Asinari [14,15] followed a similar approach to calculate PV deployment potential in Turin, in northwest Italy. Using building footprints, high-resolution DOPs, and an image recognition algorithm, they identified suitable rooftop areas. They used the solar radiation data at a 1 km resolution, as available in PV-GIS, instead of the average solar radiation data for the whole municipality. As in Ref. [13], their final PV potential results were cumulated to a city scale. Mainzer et al. [16] used OpenStreetMap to retrieve the sizes and locations of all buildings in the area of interest. Next, they applied a series of image processing algorithms to retrieve roof ridgelines and deduce the orientation of partial roof areas. Some solutions use high-resolution DOPs and machine learning techniques to retrieve suitable areas or determine solar irradiance. Assouline et al. [17], Mohajeri et al.[39], Miyazaki et al. [40], and Dwivedi et al.[41] developed Dwivedi et al. [41] developed a machine learning technique to spatially extrapolate weather variables and estimate roof characteristics from high-resolution satellite images. They used a combination of support vector machines and GIS to estimate the rooftop solar PV potential for urban areas. The main limitation of these solutions lies in the datasets needed to train the model, which consist of an enormous amount of meteorological data.

2.4. High spatial resolution

Kodysh et al. [18] employed LiDAR to generate a 1 m DSM for Knox County, TN, USA. They used this DSM as input for the ArcGIS Solar Analyst and calculated monthly average days of solar radiation to develop a cadastre of total yearly solar radiation. Hofierka and Kaňuk [19] combined a DSM with a buildings' footprint vector data with information on height to generate a DSM with 1 m resolution for Bardejov, Slovakia. They used r.sun with PV-GIS data to calculate the real-sky solar radiation and PV potential for the case-study area. The researchers performed a coarse calculation estimating that PVs could cover 2/3 of the city's electricity demand. Brito et al. [20] combined LiDAR data and photogrammetric methods to generate a 1 m DSM of a part of Carnaxide, Oeiras, Portugal. They performed the clear-sky solar radiation calculation with ArcGIS Solar Analyst and approximated real-sky conditions with PV-GIS data. Nguyen and Pearce [21] used LiDAR data of a part of downtown Kingston, ON, Canada, to generate a 55 cm DSM. They used r.horizon to speed up the solar radiation calculation and evaluated the differences in the results due to DSM resolution, the presence or absence of shadows, and the temporal granularity of the estimation. Agugiaro et al. [22] examined the solar radiation potential and created a WebGIS platform for evaluating PV potential in Trento, Italy. They used a LiDAR-derived 1 m DSM together with local imagery and advanced automated image-matching methods to generate a DSM with a 50 cm resolution. They calculated the clear-sky daily sums of solar radiation and adjusted the values to real-sky conditions with the aid of seven years of measurements obtained from a pyranometer installed on a building in the area of interest. In our previous work [23], we used a high-resolution DSM (25 cm) to recognize and exclude encumbrances on rooftops, such as chimneys and dormers. Moreover, Ref. [23] takes into account real-sky conditions by using real weather data to compute incident solar radiation on the tilted surface of rooftops and to estimate PV performance and energy production.

2.5. Energy demand integration

The analyzed solutions in the literature do not estimate energy demand. Indeed, a design for an advanced power infrastructure cannot disregard a suitable consideration of both energy generation and consumption. Both Litjens et al. [24] and Ramirez Camargo et al. [25] designed a spatiotemporal framework to evaluate the electricity demand that can be fulfilled by PV energy. For the demand side, they used a combination of household statistics, historical residential demand time series, and annual electricity consumption from residential grid connections. Groppi et al. [26] proposed a model that analyzes the evolution in energy demand after the installation of both PV and solar thermal systems. They used calculations derived from an analysis of building construction age class to evaluate the average consumption for each consumer typology. Luthander et al. [27] proposed a solution that focuses on determining how self-consumption from residential PV systems can change by using shared or individual power grid connections. They used consumption data from 21 detached single-family houses over one year with a time resolution of 10 min. All the analyzed methodologies consider the urban context in a spatiotemporal framework, taking into account both energy generation and consumption. However, most of the solutions in the literature rely on data from grid operators, standard load profiles, or models for certain typologies of users. None of them deal with realistic models of the activities and behaviors of house inhabitants or with an accurate estimation of the distribution of heterogeneous families.

2.6. Full-service platforms

Finally, a wide range of solutions—both proprietary and open-source—are used for microgrid optimization and RES systems simulation. Girardin et al. [28] developed the EnerGIS platform to evaluate integrated energy conversion systems in urban areas. Their models compute heat and electricity demand for a geographical area, evaluating building heating and cooling loads as a function of outdoor temperature. DerCAM is a techno-economic optimization model, which provides as a result, for example, the lowest-cost configuration of DG technologies for a specific building [29]. Robinson et al. [42] developed SUNtool, a planning platform that considers energy supply, demand, and user behavior under uncertainty. The user selects the global location of the area of interest, and the software retrieves both climate data and a specific dataset containing detailed attribution information for buildings as a function of age, type of use, and occupancy. Alhamwi et al. [30,43] presented an open-source GIS-based platform called FlexiGIS for the optimization of UES. FlexiGIS uses a systematic approach for a bottom-up simulation of urban electricity supply and demand down to the building unit level. City Energy Analyst [31] is an open-source software for the analysis of building energy systems at neighborhood and district scales. The software reproduces hourly PV generation profiles on rooftops with low discretization (2 m), not accounting for shadowing and encumbrances. The model that generates the energy demand profiles uses a hybrid approach in which data from local building archetypes are used as an input of a dynamic building energy model. These analyzed solutions are designed to reproduce microgrids as a whole, providing a general overview of many aspects involved in energy systems. This generality can result in poor resolution and specific capabilities. None of

the aforementioned solutions relies on shadow analysis or real-sky considerations.

2.7. Scientific contribution

The field of spatiotemporal modeling of RES potentials is only in its early development stage, and emphasis has been placed on either models with a large spatial coverage, such as entire countries, or the study of small areas, such as buildings or neighborhoods. These developments are still insufficient to support the planning process of DG systems for municipalities, and further research is necessary. Models with a low spatiotemporal discretization, which are usually available for large areas, can only be used for optimization purposes when dealing with UES. In particular, reliable methodologies are still missing for the modeling of rooftop PV electricity generation potentials and electricity demand at the urban scale in a high spatiotemporal framework. The main gaps encountered in the literature can be summarized as follows:

- Using proprietary data sources;
- Using low spatiotemporal resolution (focusing only on one aspect involved in the energy system);
- Not considering real-sky conditions and shadowing effect for the solar radiation analysis;
- Needing for a huge amount of data to train the model;
- Dealing with standard non-realistic models and load profiles.

In this paper, we introduce a novel methodology to cover the shortcomings of previous contributions in this area. Our methodology integrates reliable GIS-based PV potential assessment procedures with models to estimate both electric generation and consumption profiles. As shown in Table 1, our model relies on a high spatiotemporal resolution (25 cm and 10 min, respectively) and considers both the shadowing effects and the real-sky conditions for the solar radiation estimation. To do so, real weather data, considering clouds and real weather conditions, are used to compute incident solar radiation on the tilted surface of rooftops and to estimate PV performance and energy production. We have created an innovative infrastructure that co-simulates rooftop PV production and households' electricity demand. The proposed solution integrates open data and models with different urban geometric characteristics (e.g., census data and real weather parameters) in a GIS environment. Our infrastructure involves realistic models of the activities and behaviors of house inhabitants and performs an accurate estimation of the distribution of heterogeneous families. It integrates with the UES design methodologies to estimate energy demand with high temporal resolution, accounting for realistic populations with realistic consumption profiles. Such a powerful co-simulation environment makes it possible to perform a wide range of different simulations. The end user can define the desired granularity for the co-simulation, in terms of both spatial resolution (from a single household to an entire city) and temporal resolution (from a few minutes to days or months). This methodology allows concrete recommendations to be made in order to promote the knowledge and comprehension of UES and the integration of RES in the context of future smart cities [44,45]. In addition, it enables further considerations on the design and the maintenance of an REC (e.g., quantitative analysis of decentralized storage systems scenarios, considerations on the strengthening of the distribution network).

3. Proposed platform

In this section, we describe a spatiotemporal modeling approach that addresses the gaps described in Section 2 to promote renewable energy generation planning. We propose a GIS-based distributed software infrastructure that can co-simulate both electricity demand and supply for the area of interest. The methodology identifies suitable areas for RES exploitation (e.g., the roofs of industrial settlements and residential buildings) in relation to the surrounding area, the real RES availability, and the existing environmental and landscape constraints.

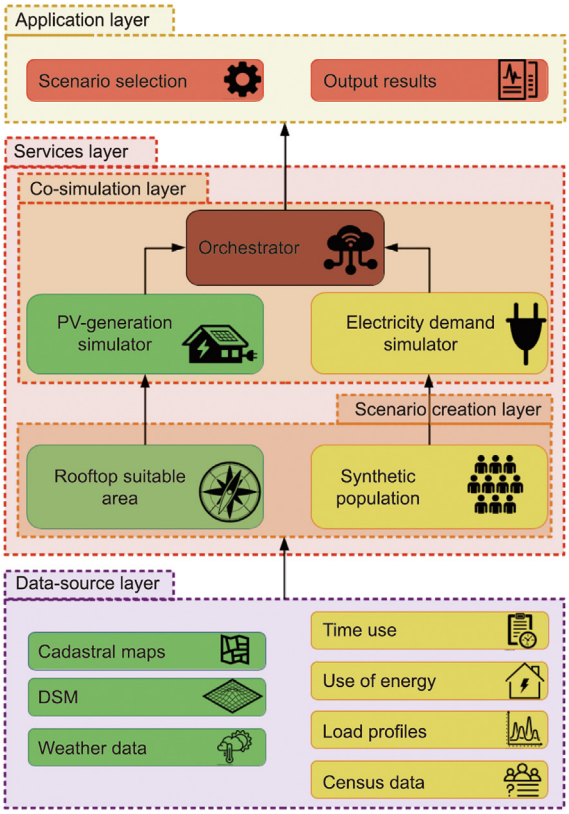

Fig. 1. Schema for the proposed co-simulation platform.

The infrastructure is developed to be distributed across different computer systems (i.e., servers and/or cloud systems), following a service-oriented design pattern [46]. In this approach, each service is highly decoupled and focused on performing a single task. This is a paramount characteristic when designing modular and flexible solutions, in order to model and co-simulate different energy flows in a single solution [47].

This work combines and extends the methodologies developed by our two previous works [23,48], by providing:

- A flexible and adaptable spatial discretization, which can be expanded from a single building to an entire city.
- A flexible and adaptable temporal discretization, which can simulate intervals from 10 min to an entire year.
- An advanced co-simulation environment, which combines both production and consumption simulations.
- Increased methodological reliability, by integrating other developed simulation tools (introduced in the next sections).

The schema represented in Fig. 1 highlights the main functional layers of the proposed methodology. The architecture of the platform begins by reproducing the urban energy infrastructure within the area of interest (the data-source layer). In this layer, raw urban input information is imported (e.g., DSM, cadastral maps, time use, and census data). In the services layer, the input data sources are first processed and filtered to create a geo-referenced dataset; next, the spatial and temporal distributions of electricity demand and supply are simulated and validated. In the application layer, the aggregation geometry and the main output results are defined

by the end user. The flexibility of the platform allows the end user to obtain results at different geographical resolutions and with different temporal discretization. The rest of this section describes each layer in detail.

3.1. Data-source layer

The data-source layer (the lower layer in Fig. 1) imports all the necessary input datasets into the infrastructure to simulate PV generation and residential load consumption. A key element of our infrastructure is to use open data whenever possible.

A cadastral map contains information about the land area (e.g., boundaries, ownership, and occupancy). It consists of a set of shapefiles covering the whole extension of the city. A shapefile is a particular form of vector data composed of a geo-referenced layer with geometrical features, such as dots, lines, or polygons. Each polygon provides its relative attributes (e.g., intended use and surface area) and the Cartesian coordinates of its vertices in the adopted reference system.

A DSM with a high resolution (less than 1 m) makes it possible ① to define the exact slopes of rooftops, ② to better recognize encumbrance on rooftops, such as chimneys and dormers, that will not allow the deployment of PV panels, and ③ to obtain a better simulation of the shadows that will affect the PV energy production. Thus, the higher the DSM resolution, the greater the accuracy of the energy production estimation.

The real weather data needed by our methodology are solar radiation and air temperature, which are used to compute energy production estimation (i.e., solar radiation for PV systems) and energy consumption (i.e., domestic lighting according to natural light). As proposed by Ref. [49], we excluded solar radiation samples with ① an altitude lower than 7° and ② a clearness index lower than 0 or higher than 1. We also excluded measured samples of global horizontal radiation with higher values than those under clear-sky conditions, again as suggested by Ref. [49].

The time use (TUS) survey provides statistical information at 10 min intervals on the activities and behaviors of inhabitants of all ages and genders; moreover, this information can be grouped by type of day (i.e., weekdays or weekends) [50,51]. TUS data is used to build a user-activity model that simulates the activities and behaviors of individual household members and, as a consequence, their respective electricity consumption at home (Section 3.2.2).

The use of energy survey gives an overview of energy consumption [52] and provides a statistical distribution of different appliances according to family size. In particular, it provides the percentage of use of electric appliances, grouped by weekdays and weekends. Our methodology exploits statistics on the distribution and usage of appliances to build a virtual and realistic population for simulation (Section 3.2.1). It associates a consistent set of appliances together with their respective percentage of use in each virtual family.

Our methodology exploits the load profiles of real appliances, which were collected by sampling different appliances with a 1 Hz resolution. The use of sampled load trends makes the whole multiscale model flexible in terms of easily including further appliances with different characteristics (e.g., load size, model, brand, and production year). For example, two similar virtual families can have a similar set of appliances with different characteristics and hence different load profiles. In such a scenario, the aggregated household load consumption of both families is different.

Census data typically provides statistics on families and populations. In the present work, we used information from census data to generate a synthetic population consisting of heterogeneous and statistically consistent families (Section 3.2.1).

3.2. Services layer

The services layer (the middle layer in Fig. 1) consists of two sub-layers: ① the scenario creation layer and ② the co-simulation layer. The services layer integrates the input data sources provided by the data-source layer to correlate them and create a geo-referenced dataset (the scenario creation layer), which is then used to feed all the simulation modules needed by the whole infrastructure (the co-simulation layer). In this section, we analyze in detail the structure of these sub-layers.

3.2.1. Scenario creation layer

The scenario creation layer creates the scenario geo-referenced dataset. To produce the data structure needed by the simulators, two main functions are performed: ① defining the rooftop suitable area, which is needed to allow the PV-generation simulator to perform a high-resolution spatial assessment of PV systems, and ② generating the synthetic population, which is needed to allow the electricity demand simulator to reproduce realistic and reliable building load profiles.

To calculate the potential of rooftop PV systems with a high spatiotemporal resolution, the first step is to identify areas where PV generation plants could be placed. Therefore, objects such as dormers and chimneys must be excluded from the analysis, by exploiting high-resolution DSM and cadastral maps coming from the data-source layer. As previously mentioned, we integrated and extended our previous work [23] to estimate the rooftops' suitable areas. The surface areas of a roof are classified based on the inclination and orientation [53], which are the two main construction factors affecting the energy production of PV systems. Within this work, we identify areas representing tilted rooftops with an orientation (γ) between 135° and 235° (oriented between the southeast and southwest) and with a slope (θ) between 10° and 45°. However, the end user can give new ranges as input for γ and θ in order to select the desired suitable surfaces.

From the resulting map, we remove small areas that are too small for installing a PV system (i.e., areas where deployable PV systems are smaller than 1 kilo Watt peak (kWp)). To select only areas belonging to building rooftops, the resulting map is clipped with the building shapes in the cadastral map. The end user can define the required simulation constraints. In addition, the type of building being considered for PV installation can be selected (e.g., residential buildings, industrial buildings, and offices). Finally, we exclude from the computation those buildings that are not suitable for a hypothetical installation of PV systems, considering the buildings' intended use and avoiding historical buildings.

A synthetic population is a simplified microscopic representation of an actual population. The synthetic population matches the aggregated statistical measures of the actual population, so the synthetic population is a realistic depiction of the real population. Households and persons are selected from random samples such that the joint distribution of their attributes of interest (e.g., age, gender, and work) match the known aggregate distributions available through census data. At its core, the synthetic population module implements PopulationSim [54], a tool that is part of the open-source collaborative framework ActivitySim [55]. The synthetic population module is used as an extension of Ref. [48], by feeding the electricity demand simulator with a realistic population (Section 3.2.2).

PopulationSim receives three main inputs, which the end user can define via comma-separated values (CSVs) files:

(1) **Seed tables:** These are composed of two lists representing households and persons for each selected seed geography (i.e., geographical discretization chosen by the end user). They are produced from census data and describe the composition of a

random sample of the population, specifying the required number of attributes for each entity. The attributes employed in this work comply with the classes of users needed by the electricity demand simulator (e.g., part-time working male, full-time working female, and child).

(2) **Marginal table:** This represents the reference marginal distribution. It comes from the census data and describes the composition of the target geography. It is divided into sub-regions (e.g., census tract and districts), and provides a detailed composition of households and persons for each sub-region.

(3) **Control variables:** This is a logical map that describes all the attributes of interest and the related path to establish their values from the various seed tables.

The main output of the synthetic population is a JSON file describing, for each household, the inhabitant composition, which assigns to each virtual person (with the corresponding attribute of interest) a virtual house in a geographic area.

3.2.2. Co-simulation layer

The co-simulation layer provides different simulation modules and defines a common structure, synchronizing and enabling communication among the different software components. Each model of the co-simulation layer consists of different software modules. It is worth noting that we designed our solution to be ready for further integration with third-party software components. Each module can eventually be invoked, even by third-party software, to retrieve information and simulation results.

The PV-generation simulator estimates the PV energy production on suitable areas on rooftops. We followed and extended the methodology of the PV-Sim proposed in our previous work [23]. The PV-generation simulator computes solar irradiance in high spatiotemporal resolution for each suitable area identified in the scenario creation layer. Following this methodology, we computed sub-hourly clear- and real-sky solar radiations. To compute clear-sky solar radiation, the PV-generation simulator produces a set of direct and diffuse solar radiation maps with 10 min time intervals. To compute real-sky solar radiation, it simulates the incident radiation on the tilted surface of buildings, considering real meteorological data coming from third-party services, such as Weather Underground [56]. The inputs needed by the simulation module are ① the suitable areas retrieved by the rooftop suitable area module and ② weather data on the outdoor air temperature and solar irradiance under real-sky conditions. Then, the PV-generation simulator estimates the PV productions for the analyzed geometry. To calculate the output power, real meteorological data are used to estimate the air and PV-cell temperatures. In addition, we used the characteristics of commercial PV modules as default values (i.e., efficiency and temperature coefficient). However, before performing the simulation, the end user can change these parameters, depending on the characteristics of the PV system of interest. The final output of the simulator is a GeoJSON that provides information for each building on the size of the deployable PV system and the related generation profiles (with a 10 min time-step) for the requested simulation period.

The electricity demand simulator simulates households' electricity load profiles. It is centered on our previous work Home-Sim [48], which is a bottom-up multiscale model to simulate energy consumption trends with different spatiotemporal resolutions. Home-Sim exploits a Monte Carlo non-homogeneous semi-Markov model that takes into account both the probability of performing an action at a certain time of day and the duration of the action itself, and that provides ① a realistic model of the activities and behaviors of house inhabitants and ② an accurate estimation of the distribution of heterogeneous families with appliances. The simulation accuracy of the model depends on the level of detail provided by the dataset that describes the population of the analyzed area of interest. To this end, instead of using raw census data, as in our previous work [48], we integrated the synthetic population generated in the synthetic population module of the scenario creation layer, thereby providing a realistic, geo-referenced, and detailed distribution of both households and persons. The inputs needed by the simulation module are ① the synthetic population generated by the synthetic population module; ② TUS surveys that include information on 12 different classes of users (e.g., part-time working male, full-time working female, and child) [57]; ③ surveys on energy use that provide the distribution of appliances according to family size and statistics on the usage of household appliances in families [52]; and ④ load profiles of real appliances sampled at 1 Hz [58]. Once the house inhabitants are grouped into specific categories, each activity is associated with one or more appliances that have been modeled following a stochastic methodology. This information is used by the platform to produce a GeoJSON that provides realistic residential load profiles (with a 10 min time-step) for either weekdays or weekends, with multilevel aggregation.

The orchestrator ① synchronizes and coordinates the different simulators and ② geo-references their inputs and output results in a common GIS environment. Fig. 2 reports the orchestrator work-flow. The co-simulation platform uses simulators in a common context to perform a coordinated simulation of the defined scenario. Thus, all simulators involved in a simulation scenario run their own processes with their own event loops. As shown in Fig. 2, the first task is to perform a geospatial classification of all the data structures, following the geographical discretization and the connections defined in the scenario selection module of the application layer. Each piece of input data is connected to the

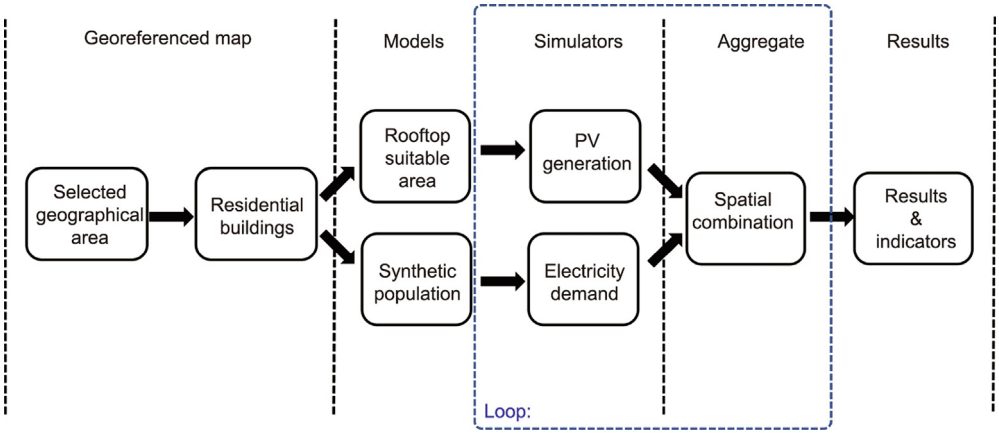

Fig. 2. Orchestrator work-flow.

others in the chosen reference geometry. The orchestrator receives the raw data from the data-source layer as input and geographically connects them to create a geo-referenced map (see "selected geographical area" and "residential buildings" in Fig. 2). For each selected area, it associates several buildings and, for each building, it associates a set of models (see "rooftop suitable area" and "synthetic population" in Fig. 2). Each geographical point has the specific attributes needed to calculate both the electricity production and the electricity demand. Therefore, building PV generation is directly connected with the electricity demand of the associated families and households. All the models run on the corresponding simulators (see "PV generation" and "electricity demand" in Fig. 2). In this way, at each time-step, the orchestrator requests each simulator to run its stand-alone calculations in a loop, producing the power values associated with its model. Within the same time-step, the orchestrator spatially aggregates the single output according to the selected geographical discretization (e.g., city district, municipality), thus obtaining a set of values that does not refer to the specific module results (e.g., single household consumption, single PV system production) but is aggregated over the selected geographical discretization (see "spatial combination" in Fig. 2). At the end of the whole co-simulation process, the final output is a set of aggregate values that can correspond to energy or power indicators (see "results & indicators" in Fig. 2).

3.3. Application layer

The application layer represents the upper layer of the proposed infrastructure (Fig. 1). It is dedicated to end-user applications, and it can provide information about performed simulations with different levels of detail. With the scenario selection module, the end user can define the different requirements to simulate the desired scenario by providing: ① the geographical area, by providing the effective shapefile and connecting it to the OpenStreetMap environment; ② the spatial and temporal resolution (from a single household to an entire city and from a few minutes to days or months, respectively), in respect to the provided data source; and ③ the technical specifications of the different modules.

The output result module is composed of the main result values and indicators. At each time-step, the main outputs of the co-simulation platform are ① the electricity demand (P_{load}), ② the PV power production (P_{prod}), ③ the directly self-consumed power (P_{self}), and ④ the not-consumed injected power (P_{inject}). P_{self} is the share of P_{prod} that can be directly consumed by the selected area, as a result of P_{load}. P_{inject} is the share of P_{prod} that overcomes P_{load}; for that reason, it can be injected into the distribution grid or into a proper energy storage system. Algorithm 1 outlines the logic behind the calculation of such values.

Algorithm 1. The logic behind the calculation of such values.

if $P_{prod} < P_{load}$:
  $P_{self} = P_{prod}$
  $P_{inject} = 0$
else $P_{prod} \geq P_{load}$:
  $P_{self} = P_{load}$
  $P_{inject} = P_{prod} - P_{load}$

It is important to emphasize that the described procedure to determine both P_{self} and P_{inject} is performed at each time-step. This particular condition makes it possible to simulate the actual self-consumed electricity, reproducing the realistic performance of an REC that, instant by instant, "understands" whether it can consume the energy it has produced, or if it needs to obtain energy from the distribution grid.

At the end of the whole co-simulation, the main aggregated values are ① the amount of absorbed energy (E_{load}), ② the energy generated by PVs (E_{prod}), ③ the self-consumed energy (E_{self}), and ④ the energy that could be injected (E_{inject}). The first two indicators make it possible to characterize a given geographical area in terms of its PV potential and REC potential. Regarding the last two values, as before, it is important to highlight that they are not a mere integral subtraction of final energies; rather, they are calculated at each time-step as the difference of instantaneous powers. Those values well represent the energy exchanges that are generated in the same selected geographic area. For that reason, the platform's ability to produce these results enables further consideration of the design and the maintenance of an REC (e.g., dimensioning and location of storage systems, strengthening of the distribution network).

To better understand the obtained results, two temporal PV integration indicators are assessed: the self-consumption ratio (SCR) and the self-sufficiency ratio (SSR) [59,60]. The SCR is used to quantify the share of electricity that is self-consumed from the total annual produced PV energy. The SSR quantifies the share of electricity consumption that is fulfilled by PV electricity. A more exhaustive definition of these indicators is provided in Appendix A Section S1.

One last indicator concerns the avoided CO_2 emissions. The residential sector is responsible for 27 % of primary energy consumption [61] and accounts for a large amount of CO_2 gas production. In 2018, the European Parliament affirmed that "the building stock ... is responsible for approximately 36% of all CO_2 emission in the European Union" [62]. For this indicator, a more exhaustive definition is given in Appendix A Section S1.

3.4. Replicability

The novel methodology presented in this manuscript can be used to assess the PV integration on building rooftops as well as analyze households' electricity demand. Within this research work, we tested the methodology in an urban context, but it can be applied to many other energy systems. By providing the requested input information, the co-simulation process can be easily replicated in other realities, such as city districts, rural areas, or entire cities. The data source layer (Section 3.1) describes in detail all the input data needed by the platform to simulate the desired scenario. Most of these data are open and easily accessible for several locations. In Europe, Eurostat provides many of the requested surveys [63]. The resolution of the final output of the simulation process is strictly correlated to the resolution of the initial input data sources.

4. Experimental results

To test and validate the simulation of the proposed software infrastructure, we selected the municipality of Turin as a case study. Turin is a city located in Piedmont, in northwest Italy. It covers an area of about 130 km^2 and has a population of over 875 000 inhabitants [64]. A detailed description of both the geography of the location and the adopted dataset is provided in Appendix A Section S2. The minimum area selected for the simulation coincides with the census tract defined by the Italian National Institute of Statistics (ISTAT) [64]. For each of the 3710 census tracts composing the municipality of Turin, the entire co-simulation procedure described in Section 3 was applied. An in-depth analysis of both energy results and indicators was performed, highlighting the major strengths and weaknesses according to the evaluated geometry. As explained in Section 3, for the demand side of the platform, calculations are only applied to residential buildings.

For the production side, a distinction was made between two different scenarios: ① Scenario RES considers only the energy that can be produced using the available surfaces of residential rooftops, while ② Scenario TOT considers the energy that can be produced using all available rooftop surfaces, including all possible buildings, both residential and non-residential. Both scenarios exclude buildings that are not suitable for PV installations, such as historical buildings, churches, or bell towers. Scenario TOT is considered as if the energy produced by all the rooftops of the census tract could be directly consumed by its residential buildings. This simplification allows us to assess how an REC can share its energy production, even though we are conscious that many other parameters (e.g., electricity distribution network and energy storage systems) might be considered to describe the effective settlement.

The results from the production side of the platform were compared with those obtained by Bergamasco and Asinari [15], whose work we consider to be a benchmark, allowing a fair comparison of the very same geographical area. Their methodology is also applied to the municipality of Turin, and it calculates the energy that might be produced by deploying a widespread rooftop PV system. In comparison with our work, they only simulate the PV production, and do not evaluate the actual population or the effective electrical consumption. As described in Section 2, they exploit image recognition algorithms to retrieve building rooftop shapes from high-resolution DOPs. For solar radiation, they use the yearly irradiance values produced by PV-GIS with a 1 km resolution, considering only clear-sky conditions [10]. In comparison with their methodology, as explained in Section 3, we calculate the solar radiation with a higher spatiotemporal resolution (10 min and 25 cm) and consider both clear-sky and real-sky conditions. We use their results as a benchmark for the production side of our methodology; the obtained enhancements are discussed in Section 4.1.

The rest of this section presents the experimental results, highlighting the flexible capabilities of the platform, first at the district level (Section 4.1), to better understand geographical distribution and dependencies. This first analysis highlights the capabilities of the co-simulation process over the entire year. Then, Section 4.2 discusses the experimental results at the census tract level, to emphasize the local performance of the platform. This second analysis highlights the capabilities of the co-simulation process up to the daily simulation.

4.1. Energy performance at the district level

Table 2 (Scenario RES) and Table 3 (Scenario TOT) report in detail the main results at the district level. In these tables, data on technical information, energy aggregated results, and energy indicators are summarized for each district in Turin. For both scenarios, beyond the individual district results, a final summarizing line reports the aggregated values for the whole municipality. Both tables show that the electricity consumption for the residential sector for the whole municipality of Turin, calculated over a population of about 860 000 inhabitants, is around 592 $GW{\cdot}h{\cdot}a^{-1}$. As explained in Section 3, this value is calculated over a realistic population that aligns with the available census data and simulates realistic load profiles for household appliances.

Table 2 describes the Scenario RES and reports that the estimated total amount of produced energy is around 353 $GW{\cdot}h{\cdot}a^{-1}$. The total available rooftop area for this scenario is 1.9 km^2. Table 3 describes the Scenario TOT and reports that the total amount of estimated energy produced is about 685 $GW{\cdot}h{\cdot}a^{-1}$, using an available rooftop surface of 3.7 km^2. This area includes non-residential rooftops as well, such as schools, shops, and factories.

Those integral results were compared with the results produced by Bergamasco and Asinari [14,15], and discrepancies and similarities between the two methodologies were identified. We divide the comparison between the area definition side and the power production side. For the area definition side, the two methodologies are compared. Bergamasco and Asinari calculated that, for the whole municipality of Turin, 43 500 residential buildings had 1.7 km^2 of suitable area for PV installation. Our result, in Scenario RES, is quite similar, identifying about 45 000 buildings and 1.9 km^2 of available surfaces. For the power production side, we can affirm that our simulation presents increased considerations of the time dependencies of both solar radiation and real weather data. Beyond that, a comparison between the effective PV potentials was made. Bergamasco and Asinari reported final results only for the whole municipality level, indicating that it could produce about 600–800 $GW{\cdot}h{\cdot}a^{-1}$, depending on PV panel typologies. We compare here the Scenario TOT production result, which is about 592 $GW{\cdot}h{\cdot}a^{-1}$.

Another interesting observation involves the avoided CO_2 emissions indicator. As explained in Appendix A Section S1, this indicator is in proportion to the PV energy production (E_{prod}), and does not consider the direct use of the energy produced. The simplification assumed with this hypothesis is that all the energy produced by PV systems avoids being produced by traditional pollutant fossil-fuel systems. With this premise, we can observe that the maximum reduction of CO_2 emissions is obtained where the energy production is maximized—namely, the Centro district for the Scenario RES (14 $Mt{\cdot}a^{-1}$) and the Mirafiori Sud district for the Scenario TOT (45 $Mt{\cdot}a^{-1}$).

Fig. 3 summarizes, with a comprehensive bar plot, the distribution of energy production and energy demand within the districts of the municipality of Turin. The plot depicts both energy consumption and production, emphasizing the differences between Scenario RES and Scenario TOT. It clearly shows that, for certain districts (e.g., Mirafiori Sud and Falchera), the difference between Scenario RES and Scenario TOT can reach high amounts. This is because large factories are located in these districts which—if used for PV installation purposes—would allow the production of a significant amount of electrical energy. It can also be seen that, for certain districts, just the E_{prod} from residential buildings (Scenario RES) would be sufficient to supply the E_{load} of the whole district. In particular, five districts (i.e., Barca, Borgo Po e Cavoretto, Centro, Falchera, and Madonna del Pilone) might produce more electricity than they consume with only Scenario RES. In contrast, five districts (i.e., Aurora Porta Palazzo, Madonna di Campagna, Mirafiori Sud, Regio Parco, and Vanchiglia) can only overcome their electrical consumption with Scenario TOT. Finally, for 15 districts (i.e., Barriera di Milano, Borgata Vittoria, Cenisia, Crocetta, Lingotto Filadelfia, Mirafiori Nord, Nizza Millefonti, Parella, Pozzo Strada, Rebaudengo, San Donato, San Paolo, San Salvario, Santa Rita, and Vallette Lucento), their total electrical consumption cannot be supplied by PV systems, even if the whole available rooftop surface were to be used.

The spatial dependency of the SCR and SSR has been accurately analyzed, and the results are reported in Appendix A Section S3.

4.2. Energy performance at the census tract level

In this section, the experimental results are discussed for three significant census tracts, emphasizing the platform's capability to reach a high spatiotemporal resolution. For each tract, both the energy on a monthly basis and the daily power profiles are presented for two reference days in winter and summer, respectively.

The first analyzed census tract belongs to the Parella district, which was chosen because it represents an area with a typical

Table 2
Summary table for Scenario RES.

District name	S (km^2)	Pop	Building	S_{avail} (km^2)	E_{load} ($GW{\cdot}h{\cdot}a^{-1}$)	E_{prod} ($GW{\cdot}h{\cdot}a^{-1}$)	E_{self} ($GW{\cdot}h{\cdot}a^{-1}$)	E_{inject} ($GW{\cdot}h{\cdot}a^{-1}$)	SCR (%)	SSR (%)	CO_2^{avoid} ($Mt{\cdot}a^{-1}$)
Aurora Porta Palazzo	2.74	37 342	1 381	0.08	26.47	15.25	7.74	7.51	50.77	29.26	7.37
Barca	4.43	10 891	1 835	0.06	6.62	11.08	2.70	8.38	24.40	40.84	5.35
Barriera di Milano	2.83	47 124	2 462	0.09	32.38	16.32	9.06	7.26	55.50	27.97	7.88
Borgata Vittoria	3.83	39 268	2 012	0.08	26.42	14.43	7.50	6.93	51.96	28.39	6.97
Borgo Po e Cavoretto	13.61	18 730	4 371	0.11	13.80	20.70	5.45	15.22	26.50	39.75	10.00
Cenisia	2.34	38 408	2 031	0.08	28.63	14.98	8.64	6.34	57.66	30.17	7.24
Centro	3.76	36 518	1 724	0.16	29.34	29.59	10.30	19.29	34.81	35.12	14.29
Crocetta	2.78	33 564	1 690	0.10	26.62	18.02	8.58	9.45	47.59	32.22	8.70
Falchera	12.88	11 302	798	0.04	6.37	7.26	2.26	5.00	31.17	35.53	3.51
Lingotto Filadelfia	3.60	48 560	1 178	0.07	31.23	12.48	7.87	4.61	63.09	25.21	6.03
Madonna del Pilone	15.50	14 001	3 614	0.09	10.37	16.32	4.06	12.25	24.90	39.18	7.88
Madonna di Campagna	5.28	40 984	2 294	0.08	27.55	15.52	8.12	7.40	52.30	29.47	7.50
Mirafiori Nord	3.79	43 262	1 300	0.05	25.89	9.51	5.40	4.12	56.71	20.85	4.60
Mirafiori Sud	11.35	34 197	1 733	0.08	20.42	14.27	6.02	8.26	42.15	29.46	6.89
Nizza Millefonti	3.51	27 990	979	0.04	17.99	7.10	4.88	2.22	68.73	25.69	3.43
Parella	4.91	46 282	2 873	0.09	33.51	16.57	9.08	7.49	54.78	27.08	8.00
Pozzo Strada	4.23	56 618	2 653	0.08	39.12	15.45	9.77	5.67	63.27	24.98	7.46
Rebaudengo	1.61	14 730	578	0.02	9.15	3.37	2.26	1.11	67.02	24.66	1.63
Regio Parco	2.43	16 778	557	0.03	10.88	5.97	2.93	3.03	49.17	26.96	2.88
San Donato	2.71	47 440	2 090	0.11	34.91	20.42	10.75	9.67	52.66	30.81	9.86
San Paolo	2.21	34 585	1 619	0.05	23.75	9.83	5.76	4.07	58.59	24.25	4.75
San Salvario	2.34	35 351	1 290	0.07	27.00	13.34	7.74	5.61	57.99	28.67	6.45
Santa Rita	3.57	55 903	1 769	0.10	36.76	17.86	10.59	7.27	59.32	28.82	8.63
Vallette Lucento	7.49	40 262	1 523	0.07	23.76	13.29	7.15	6.14	53.78	30.08	6.42
Vanchiglia	3.44	30 095	1 287	0.08	22.21	14.44	7.14	7.30	49.43	32.14	6.98
Turin RES	127.18	860 185	45 641	1.90	592.14	353.38	171.78	181.59	50.17	29.90	170.68

S: area extension; Pop: population; S_{avail}: suitable roof area; CO_2^{avoid}: avoided CO_2 emissions.

Table 3
Summary table for Scenario TOT.

District name	S (km^2)	Pop	Building	S_{avail} (km^2)	E_{load} ($GW{\cdot}h{\cdot}a^{-1}$)	E_{prod} ($GW{\cdot}h{\cdot}a^{-1}$)	E_{self} ($GW{\cdot}h{\cdot}a^{-1}$)	E_{inject} ($GW{\cdot}h{\cdot}a^{-1}$)	SCR (%)	SSR (%)	CO_2^{avoid} ($Mt{\cdot}a^{-1}$)
Aurora Porta Palazzo	2.74	37 342	1 959	0.14	26.47	26.34	8.71	17.63	33.07	32.91	12.72
Barca	4.43	10 891	2 360	0.11	6.62	20.25	2.82	17.42	13.95	42.68	9.78
Barriera di Milano	2.83	47 124	2 992	0.12	32.38	22.70	9.73	12.97	42.85	30.04	10.96
Borgata Vittoria	3.83	39 268	2 802	0.13	26.42	23.81	8.11	15.70	34.07	30.71	11.50
Borgo Po e Cavoretto	13.61	18 730	4 774	0.15	13.80	27.13	5.69	21.45	20.96	41.21	13.11
Cenisia	2.34	38 408	2 467	0.11	28.63	21.07	9.05	12.01	42.98	31.62	10.18
Centro	3.76	36 518	2 267	0.24	29.34	43.98	10.93	33.05	24.85	37.25	21.24
Crocetta	2.78	33 564	2 065	0.14	26.62	25.48	8.91	16.57	34.95	33.46	12.31
Falchera	12.88	11 302	1 512	0.45	6.37	82.63	2.47	80.16	2.99	38.81	39.91
Lingotto Filadelfia	3.60	48 560	1 620	0.11	31.23	19.74	8.57	11.17	43.43	27.45	9.54
Madonna del Pilone	15.50	14 001	3 965	0.11	10.37	20.62	4.19	16.43	20.32	40.42	9.96
Madonna di Campagna	5.28	40 984	3 133	0.15	27.55	28.37	9.14	19.23	32.23	33.18	13.70
Mirafiori Nord	3.79	43 262	1 686	0.10	25.89	17.93	6.06	11.86	33.82	23.42	8.66
Mirafiori Sud	11.35	34 197	2 641	0.51	20.42	93.40	6.78	86.62	7.26	33.21	45.11
Nizza Millefonti	3.51	27 990	1 454	0.07	18.99	12.90	5.42	7.48	42.01	28.54	6.23
Parella	4.91	46 282	3 524	0.16	33.51	30.25	10.03	20.22	33.15	29.92	14.61
Pozzo Strada	4.23	56 618	3 346	0.12	39.12	23.09	10.95	12.14	47.43	27.99	11.15
Rebaudengo	1.61	14 730	758	0.03	9.15	5.22	2.46	2.75	47.22	26.93	2.52
Regio Parco	2.43	16 778	833	0.06	10.88	11.88	3.21	8.67	27.00	29.47	5.74
San Donato	2.71	47 440	2 583	0.14	34.91	25.94	11.33	14.61	43.67	32.45	12.53
San Paolo	2.21	34 585	1 988	0.07	23.75	13.58	6.26	7.32	46.10	26.36	6.56
San Salvario	2.34	35 351	1 685	0.10	27.00	17.94	8.34	9.60	46.50	30.90	8.67
Santa Rita	3.57	55 903	2 224	0.14	36.76	25.38	11.32	14.07	44.58	30.78	12.26
Vallette Lucento	7.49	40 262	2 108	0.13	23.76	23.37	7.79	15.58	33.34	32.79	11.29
Vanchiglia	3.44	30 095	1 715	0.12	22.21	22.76	7.54	15.22	33.13	33.95	10.99
Turin TOT	127.18	860 185	58 461	3.72	592.14	685.76	185.82	499.94	33.27	32.26	331.22

mixture of residential and non-residential buildings, including offices, schools, and commercial buildings (Fig. 4(a)). As shown in Table 4, this census tract is populated by 587 persons living in 28 residential buildings and consuming about 273 $MW{\cdot}h{\cdot}a^{-1}$. It can be seen that, with Scenario RES, the electricity produced is not able to meet the residential energy loads. Considering Scenario

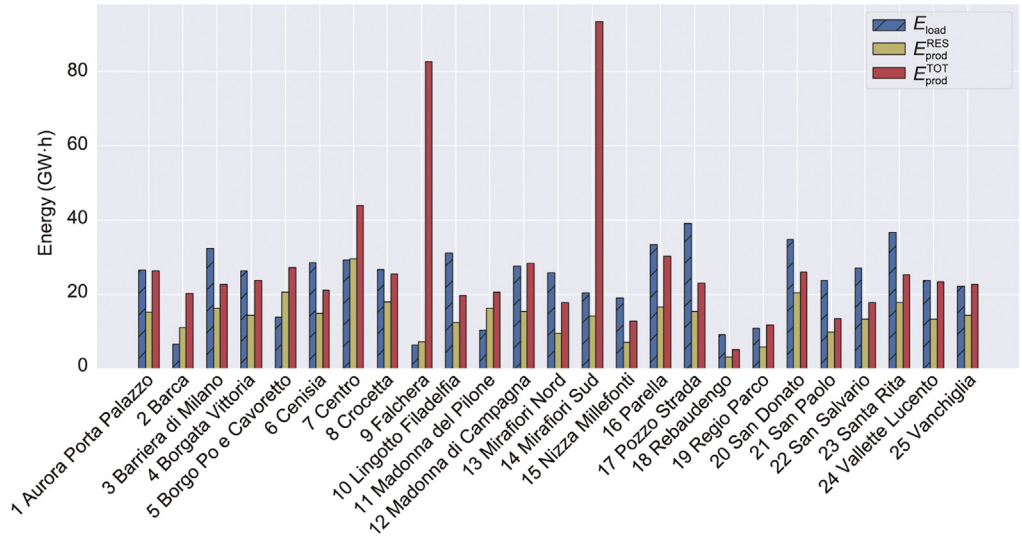

Fig. 3. District energy integrals: annual consumed energy (E_{load}) (Mt·a^{-1}), annual produced energy with Scenario RES (E^{RES}_{prod}) (GW·h·a^{-1}), and annual produced energy with Scenario TOT (E^{TOT}_{prod}) (GW·h·a^{-1}).

TOT instead (i.e., considering non-residential buildings as well), the PV production exceeds the amount of consumed electricity by about 50 MW·h. This census tract has a fairly high SCR, ranging from 65.3% in the Scenario RES to 32.8% in the Scenario TOT. Also, the SSR is slightly greater than the average value, ranging from 32.7% in the Scenario RES to 40.7% in the Scenario TOT. CO_2 emission reductions are limited, reaching at most 160 t·a^{-1}.

Fig. 4(b) gives a more comprehensive view of the energy flows occurring during the year. It can be seen that, even if the total energy produced over the year is sufficient to supply the energy needs, this situation happens only between March and September. During winter, not even Scenario TOT can satisfy the entire residential energy needs. This issue becomes even more evident in the bottom part of Fig. 4, where the daily power flows of a typical day during winter (Fig. 4(c)) and summer (Fig. 4(d)) are presented. It is clear that PV production overcomes energy loads only during daylight, whenever it is possible. For example, for a summer day when the daylight is longer, PV systems cannot directly supply the energy loads at night.

The second analyzed census tract belongs to the Madonna del Pilone district (Fig. 5(a)), which was chosen because it represents an area in which the energy production from residential buildings is maximized. Table 5 shows that this census tract is populated by 381 persons living in 151 residential buildings and consuming about 282 MW·h·a^{-1}. Here, the amount of electricity that could be produced with residential buildings exceeds the energy needs by 257 MW·h. When considering non-residential buildings as well, the excess of electricity increases to 489 MW·h. This census tract presents a relatively low SCR, ranging from 22.2% in the Scenario RES to 16.2% in the Scenario TOT. In contrast, the SSR is much higher, ranging from 42.6% in the Scenario RES to 44.3% in the Scenario TOT. A census tract with these characteristics (relatively low SCR and high SSR) is a good candidate for PV installation, which will cover almost half of the energy load; moreover, there will be many periods during the day when a surplus of PV energy production will occur. In this case, the CO_2 emission reductions are higher than in the previously analyzed census tract in Parella, reaching at least 260 t·a^{-1}.

Fig. 5(b) provides a more comprehensive view of the energy flows during the year. In this case, the monthly average energy produced is not always sufficient to supply the energy needs. However, from February to November, the energy produced in both Scenario RES and Scenario TOT can satisfy the residential energy loads. Furthermore, it is noticeable that the excess of energy produced in a year in this census tract is much greater than that of the previously analyzed census tract in Parella.

The bottom part of Fig. 5 shows the aforementioned consideration, where the PV production can provide the complete supply for the electricity load only during a certain range of daytime. During winter (Fig. 5(c)), there are fewer daylight hours, and the time evolution of the energy loads often does not align with the rooftop PV production. During summer (Fig. 5(d)), there are more daylight hours; therefore, PV production starts earlier and ends later (in addition to being more powerful). As a result, the complete electrical load can be supplied more frequently by the PV systems.

The last analyzed census tract belongs to the Falchera district (see Fig. 6(a)). As already mentioned, Falchera is one of the two industrial districts in the municipality of Turin. Thus, the analyzed census tract represents an area in which the energy production from industrial buildings is maximized. Table 6 and Fig. 6(b) show that the census tract is devoid of inhabitants and, therefore, of residential energy loads. For this reason, the energy produced with Scenario RES is equal to zero. Instead, the electricity produced with Scenario TOT appears to be very high, reaching over 62 GW·h·a^{-1}. As this census tract is devoid of E_{self}, both the SCR and SSR are equal to zero. A huge reduction in CO_2 emissions could be obtained with Scenario TOT, accounting for over 30 000 t·a^{-1}. Figs. 6(c) and (d) only show the produced energy with Scenario TOT, emphasizing the high seasonality of PV energy production.

5. Limitations and future work

In this paper, we introduced a novel methodology to cover the shortcomings of solutions in the existing literature, as described in Section 2. As pointed out in Section 3.1, the requested data sources are open and easily accessible for many locations. Nevertheless, our model relies on a high spatiotemporal resolution (i.e., 25 cm and 10 min, respectively), which allows it to identify rooftop encumbrances (e.g., chimneys and dormers) and shadows under real-sky conditions for accurate solar radiation estimation. A DSM with a lower resolution will not correctly identify such encumbrances, which will affect the identification of available rooftop surfaces and the computation of shadow evolutions. The DSM was provided by the city council and reports rooftop shapes with high accuracy, highlighting encumbrances such as chimneys and dormers. This data source has a significant production cost,

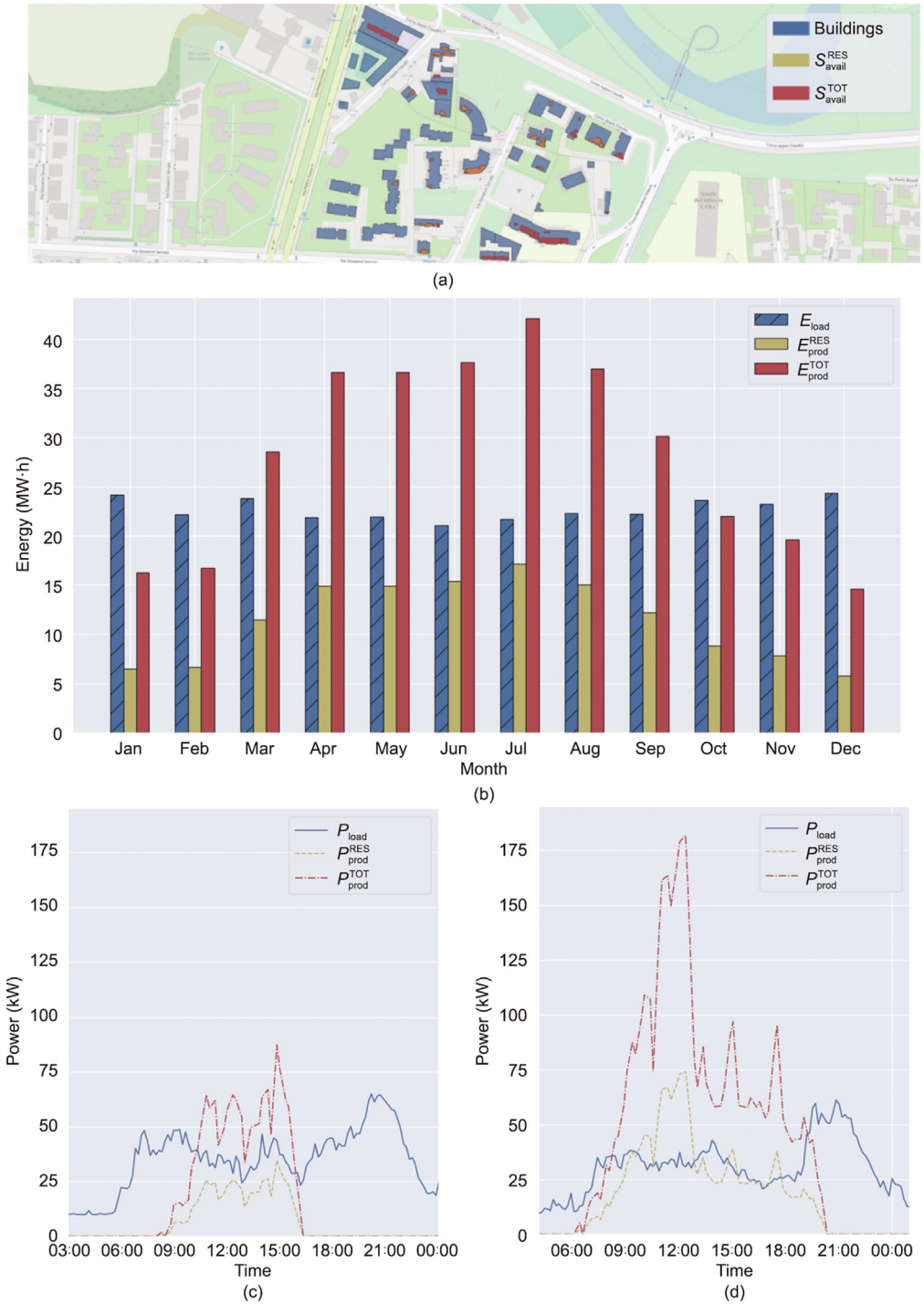

Fig. 4. Summary results for the census tract in Parella. (a) A geo-referenced representation of the available building and rooftop surfaces for Scenario RES (S^{RES}_{avail}) and for Scenario TOT (S^{TOT}_{avail}); (b) a histogram of the monthly consumed energy (E_{load}), monthly produced energy with Scenario RES (E^{RES}_{prod}), and monthly produced energy with Scenario TOT (E^{TOT}_{prod}); (c, d) daily consumed power (P_{load}), daily produced power with Scenario RES (P^{RES}_{prod}) and daily produced power with Scenario TOT (P^{TOT}_{prod}) in a reference day for the (c) winter and (d) summer seasons.

Table 4
Summary table for the census tract in Parella: Scenario RES and Scenario TOT.

Scenario	S (m^2)	Pop	Building	S_{avail} (m^2)	E_{load} (MW·h·a^{-1})	E_{prod} (MW·h·a^{-1})	E_{self} (MW·h·a^{-1})	E_{inject} (MW·h·a^{-1})	SCR (%)	SSR (%)	CO_2^{avoid} (t·a^{-1})
RES	108 032.8	587	28	727.3	272.8	136.7	89.3	47.4	65.3	32.7	66.0
TOT	108 032.8	587	41	1 775.1	272.8	338.1	110.9	227.2	32.8	40.7	163.3

so its provision is not straightforward. Nevertheless, many municipalities and city councils in Europe are producing DSMs of principal regions and cities, some created with LiDAR and some with other image reconstruction techniques.

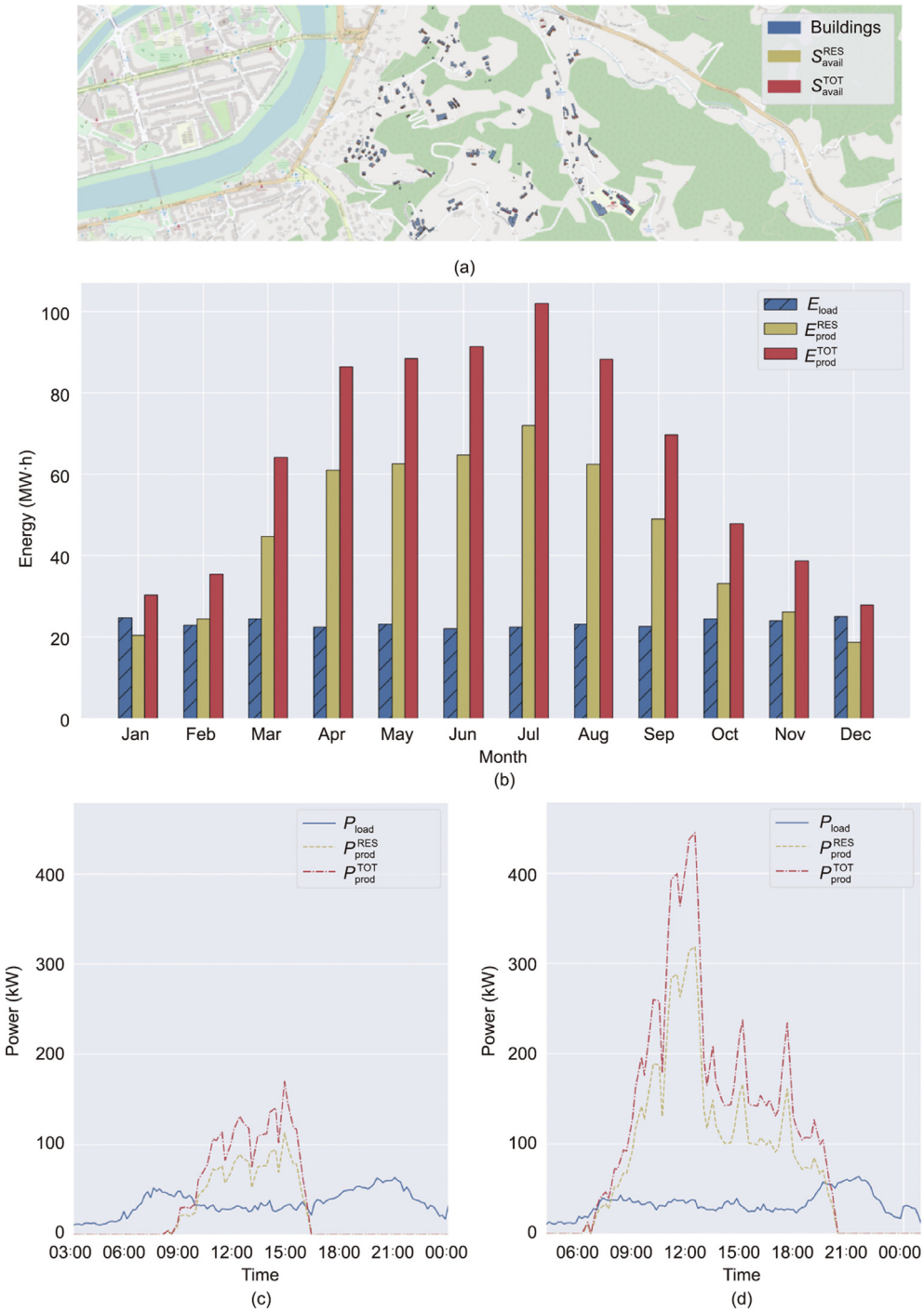

Fig. 5. Summary results for the census tract in Madonna del Pilone. (a) A geo-referenced representation of the available building and rooftop surfaces for Scenario RES (S^{RES}_{avail}) and Scenario TOT (S^{TOT}_{avail}); (b) a histogram showing the monthly consumed energy (E_{load}), monthly produced energy with Scenario RES (E^{RES}_{prod}) and monthly produced energy with Scenario TOT (E^{TOT}_{prod}); (c, d) daily consumed power (P_{load}), daily produced power with Scenario RES (P^{RES}_{prod}), and daily produced power with Scenario TOT (P^{TOT}_{prod}) in a reference day for the (c) winter and (d) summer seasons.

Table 5
Summary table for the census tract in Madonna del Pilone: Scenario RES and Scenario TOT.

Scenario	S (m^2)	Pop	Building	S_{avail} (m^2)	E_{load} ($MW{\cdot}h{\cdot}a^{-1}$)	E_{prod} ($MW{\cdot}h{\cdot}a^{-1}$)	E_{self} ($MW{\cdot}h{\cdot}a^{-1}$)	E_{inject} ($MW{\cdot}h{\cdot}a^{-1}$)	SCR (%)	SSR (%)	CO_2^{avoid} ($t{\cdot}a^{-1}$)
RES	697 381.6	381	151	3 151.0	281.6	539.9	120.0	419.9	22.2	42.6	260.8
TOT	697 381.6	381	169	4 436.8	281.6	771.0	124.8	646.2	16.2	44.3	372.4

The platform results can highlight the elements needed to design and maintain an REC, with different levels of detail (both in time and in space). The obtained results identify the exact power flows involved in the energy system, highlighting periods and locations where electricity is in excess or in defect. Such results set out a groundwork for the integration of RES and flexibilization

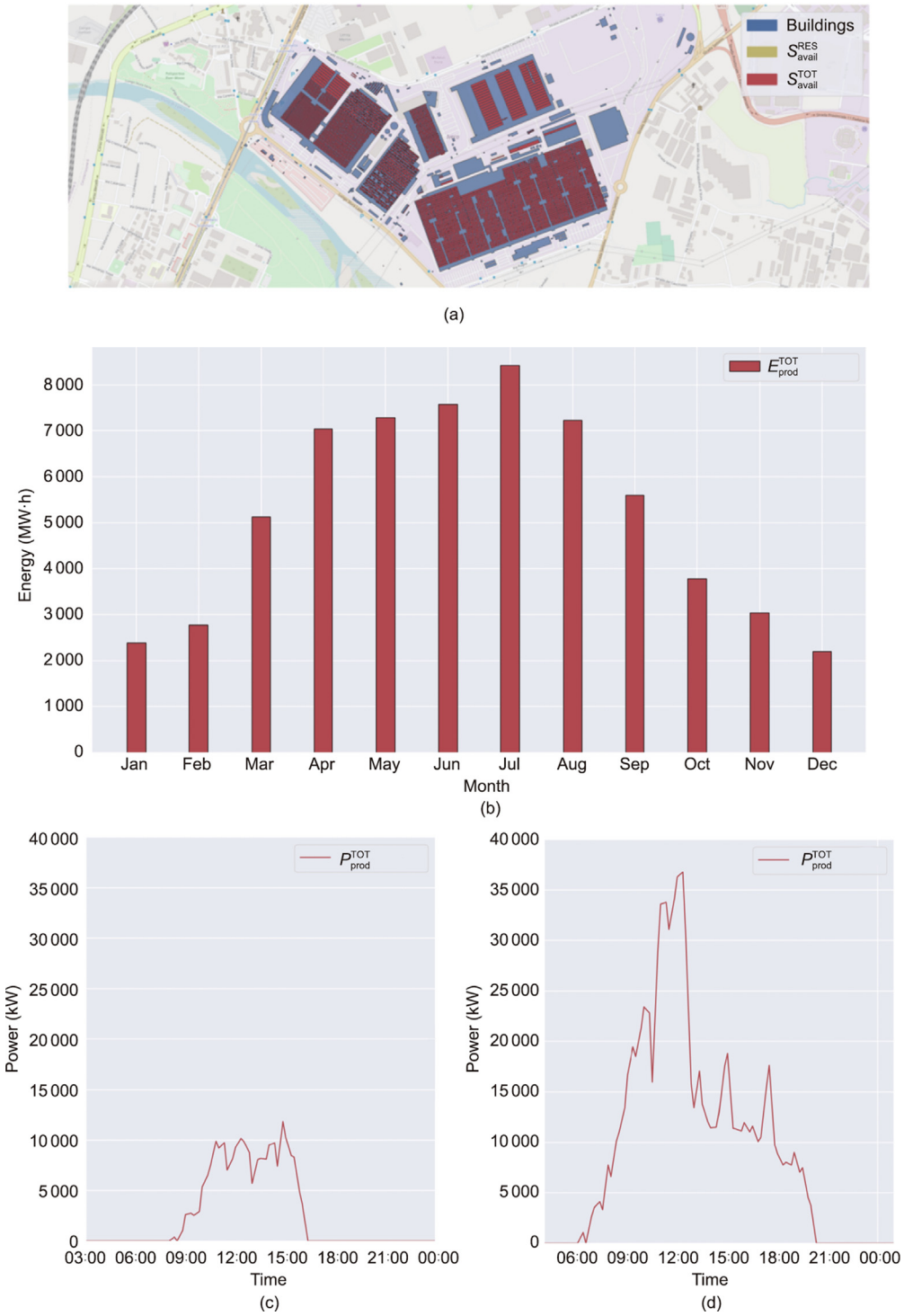

Fig. 6. Summary results for the census tract in Falchera. (a) A geo-referenced representation of the available building and rooftop surfaces for Scenario RES (S^{RES}_{avail}) and Scenario TOT (S^{TOT}_{avail}); (b) a histogram reporting monthly consumed energy (E_{load}) and monthly produced energy with Scenario RES (E^{RES}_{prod}) and Scenario TOT (E^{TOT}_{prod}); (c, d) daily consumed power (P_{load}), daily produced power with Scenario RES (E^{RES}_{prod}), and daily produced power with Scenario TOT (P^{TOT}_{prod}) in a reference day for the (c) winter and (d) summer seasons.

Table 6
Summary table for the census tract in Falchera: Scenario RES and Scenario TOT.

Scenario	S (m^2)	Pop	Building	S_{avail} (m^2)	E_{load} (MW·h·a^{-1})	E_{prod} (MW·h·a^{-1})	E_{self} (MW·h·a^{-1})	E_{inject} (MW·h·a^{-1})	SCR (%)	SSR (%)	CO_2^{avoid} (t·a^{-1})
RES	0	0	0	0	0	0	0	0	0	0	0
TOT	1 772 344.9	0	128	348 028.9	0	62 473.2	0	62 473.2	0	0	30 174.6

technologies in the context of future smart cities. Hence, they enable the analysis of the strengthening of existing distribution networks, evolving existing power grids into smart grid models [44,45]. Future works will include GIS software components for simulating and analyzing electrical distribution grids. This can only be achieved by possessing both the topological and topographical data of distribution networks, which is difficult to achieve. To meet this limitation, software such as those reported in Refs. [65–67] could be used to generate synthetic, realistic, and geo-referenced electrical distribution networks.

Moreover, the results presented here empower the design and dimensioning of storage systems, considering conventional chemical storage systems or more advanced techniques such as electric vehicles [68], demand side management, or demand response strategies. The purpose of the proposed co-simulation platform is not confined to a mere PV installation feasibility calculation; rather, it enables the performance of a wide-ranging analysis whose results can be used to foster novel energy decision-making strategies.

6. Conclusion

In this work, we proposed a GIS-based distributed software infrastructure that can co-simulate both electricity demand and energy supply for the area of interest. The methodology identifies suitable areas for RES exploitation (e.g., the roofs of industrial settlements and residential buildings) in relation to the surrounding area, the actual RES availability, and the existing environmental and landscape constraints. We have created an innovative infrastructure that co-simulates rooftop PV production and households' electricity demand. Our methodology integrates reliable GIS-based PV potential assessment procedures with models to estimate electric generation and consumption profiles. Our model relies on a high spatiotemporal resolution and considers both the shadowing effects and the real-sky conditions for the solar radiation estimation. Real weather data, considering clouds and real weather conditions, are used to compute incident solar radiation on the tilted surface of rooftops and to estimate PV performance and energy production. The infrastructure involves realistic models of the activities and behaviors of house inhabitants and provides an accurate estimation of the distribution of heterogeneous families. It integrates methodologies to estimate energy demand with a high temporal resolution, accounting for realistic populations with realistic consumption profiles. The proposed solution integrates open data and models with different urban geometric characteristics (e.g., census data and real weather parameters) in a GIS environment.

The exploitation of our software infrastructure can benefit various users and applications. Individual citizens can evaluate the economic and environmental savings that can be achieved by installing new PV systems, considering the possibility of self-supplying their domestic consumption or sharing the ownership within the neighborhoods to form an REC. Energy aggregators can use our results to identify and plan for the new capacity of PV rooftops, which is highly productive. Distribution system operators can take advantage of the proposed solution for network balancing and for planning retrofits and/or extensions of existing distribution grids. Finally, energy and city planners can evaluate the impacts of the installation of large PV systems in city districts. All these considerations are feasible, thanks to the high flexibility of the platform, which makes it possible to investigate different scenarios with different spatiotemporal resolutions. The high spatiotemporal discretization of the data sources allows end users to carry out simulations for both operational and long-term planning activities.

Within this research work, we tested the methodology in a real urban context by applying it to the city of Turin, Italy. For the whole municipality, we simulated both residential domestic loads and rooftop PV production. The electricity consumption was calculated over a realistic population, in alignment with the available census data, and simulated the realistic load profiles of household appliances. The total calculated electricity consumption for the whole municipality was around 592 $GW{\cdot}h{\cdot}a^{-1}$. The production side was divided between Scenario RES, which considers PV installation only on residential buildings, and Scenario TOT, which also considers installation on non-residential buildings. The total available rooftop area for Scenario RES is 1.9 km^2, and the estimated total amount of produced energy is around 353 $GW{\cdot}h{\cdot}a^{-1}$. In comparison, the total available rooftop area for Scenario TOT is 3.7 km^2, and the estimated total amount of produced energy is around 685 $GW{\cdot}h{\cdot}a^{-1}$.

Compliance with ethics guidelines

Marco Massano, Enrico Macii, Andrea Lanzini, Edoardo Patti, and Lorenzo Bottaccioli declare that they have no conflict of interest or financial conflicts to disclose.

Appendix A. Supplementary data

Supplementary data to this article can be found online at https://doi.org/10.1016/j.eng.2022.06.020.

References

[1] Commission E. The European Green Deal. Brussels: European Commission; 2019 Dec 12.
[2] Dóci G, Vasileiadou E, Petersen AC. Exploring the transition potential of renewable energy communities. Futures 2015;66:85–95.
[3] The European Parliament and the Council of the European Union. Directive (EU) 2018/2001 of the European Parliament and of the Council of 11 December 2018 on the promotion of the use of energy from renewable sources. Off J Eur Union 2018;L328:82–209.
[4] Caramizaru A, Uihlein A. Energy communities: an overview of energy and social innovation. JRC Science for Police Report. Luxembourg: Publications Office of the European Union; 2020.
[5] Lowitzsch J. Investing in a renewable future-renewable energy communities, consumer (co-)ownership and energy sharing in the clean energy package. Eur Energy Clim J 2020;9(2–3):45–70.
[6] Rose A, Vadari S, Wigle L. How the internet of things will enable vast new levels of efficiency. In: 2014 ACEEE Summer Study on Energy Efficiency in Buildings; 2014 Aug 17–23; Pacific Grove, CA, USA. Washington, DC: Office of Energy Efficiency & Renewable Energy; 2014. p. 295–307.
[7] Bottaccioli L, Patti E, Macii E, Acquaviva A. Distributed infrastructure for multi-energy-systems modelling and co-simulation in urban districts. In: Proceedings of the 7th International Conference on Smart Cities and Green ICT Systems (SMARTGREENS 2018); 2018 Mar 16–18; Funchal, Portugal. Setúbal: Science and Technology Publications, Lda; 2018. p. 262–9.
[8] Connolly T, College B. Understanding GIS—the ARC/INFO method [Internet]. Redlands: Environmental System Research Institute; 1992 [cited 2022 Jan 12]. Available from: http://www.ciesin.org/docs/005-331/005-331.html.
[9] Resch B, Sagl G, Törnros T, Bachmaier A, Eggers JB, Herkel S, et al. GIS-based planning and modeling for renewable energy: challenges and future research avenues. ISPRS Int J Geo-inf 2014;3(2):662–92.
[10] Suri M, Huld T, Cebecauer TÁ, Dunlop ED. Geographic aspects of photovoltaics in Europe: contribution of the PVGIS website. IEEE J Sel Top Appl Earth Obs Remote Sens 2008;1(1):34–41.
[11] HOMER [Internet]. Golden: National Renewable Energy Laboratory (NREL); 2009 [cited 2021 Mar 12]. Available from: https://www.nrel.gov/homer.
[12] Lund H, Thellufsen JZ, Ostergaard PA, Sorknaes P, Skov IR, Mathiesen BV. EnergyPLAN–Advanced analysis of smart energy systems. Smart Energy 2021;1:100007.
[13] Wiginton LK, Nguyen HT, Pearce JM. Quantifying rooftop solar photovoltaic potential for regional renewable energy policy. Comput Environ Urban Syst 2010;34(4):345–57.
[14] Bergamasco L, Asinari P. Scalable methodology for the photovoltaic solar energy potential assessment based on available roof surface area: application to Piedmont Region (Italy). Sol Energy 2011;85(5):1041–55.
[15] Bergamasco L, Asinari P. Scalable methodology for the photovoltaic solar energy potential assessment based on available roof surface area: further

improvements by ortho-image analysis and application to Turin (Italy). Sol Energy 2011;85(11):2741–56.
[16] Mainzer K, Killinger S, McKenna R, Fichtner W. Assessment of rooftop photovoltaic potentials at the urban level using publicly available geodata and image recognition techniques. Sol Energy 2017;155:561–73.
[17] Assouline D, Mohajeri N, Scartezzini JL. Quantifying rooftop photovoltaic solar energy potential: a machine learning approach. Sol Energy 2017;141:278–96.
[18] Kodysh JB, Omitaomu OA, Bhaduri BL, Neish BS. Methodology for estimating solar potential on multiple building rooftops for photovoltaic systems. Sustain Cities Soc 2013;8:31–41.
[19] Hofierka J, Kaňuk J. Assessment of photovoltaic potential in urban areas using open-source solar radiation tools. Renew Energy 2009;34(10):2206–14.
[20] Brito MC, Gomes N, Santos T, Tenedório JA. Photovoltaic potential in a Lisbon suburb using LiDAR data. Sol Energy 2012;86(1):283–8.
[21] Nguyen HT, Pearce JM. Incorporating shading losses in solar photovoltaic potential assessment at the municipal scale. Sol Energy 2012;86(5):1245–60.
[22] Agugiaro G, Nex F, Remondino F, De Filippi R, Droghetti S, Furlanello C. Solar radiation estimation on building roofs and web-based solar cadastre. In: Proceeding of the ISPRS Annals of the Photogrammetry, Remote Sensing and Spatial Information Sciences; 2012 Aug 25–Sep 1; Melbourne, VIC, Australia; 2012. p. 177–82.
[23] Bottaccioli L, Patti E, Macii E, Acquaviva A. GIS-based software infrastructure to model PV generation in fine-grained spatio-temporal domain. IEEE Syst J 2018;12(3):2832–41.
[24] Litjens GBMA, Kausika BB, Worrell E, van Sark WGJHM. A spatio-temporal city-scale assessment of residential photovoltaic power integration scenarios. Sol Energy 2018;174:1185–97.
[25] Ramirez Camargo L, Zink R, Dorner W, Stoeglehner G. Spatio-temporal modeling of roof-top photovoltaic panels for improved technical potential assessment and electricity peak load offsetting at the municipal scale. Comput Environ Urban Syst 2015;52:58–69.
[26] Groppi D, de Santoli L, Cumo F, Astiaso GD. A GIS-based model to assess buildings energy consumption and usable solar energy potential in urban areas. Sustain Cities Soc 2018;40:546–58.
[27] Luthander R, Lingfors D, Munkhammar J, Widén J. Self-consumption enhancement of residential photovoltaics with battery storage and electric vehicles in communities. In: Proceedings of the ECEEE Summer Study on Energy Efficiency: First Fuel Now; 2015 Jun 1–6; Hyères, France. Stockholm: European Council for an Energy Efficient Economy (eceee); 2015. p. 991–1002.
[28] Girardin L, Marechal F, Dubuis M, Calame-Darbellay N, Favrat D. EnerGis: a geographical information based system for the evaluation of integrated energy conversion systems in urban areas. Energy 2010;35(2):830–40.
[29] Berkeley Lab. Microgrids at Berkeley Lab [Internet]. Berkeley: Department of Energy National Laboratory Managed by the University of California; 2000 [cited 2022 Jan 12]. Available from: https://gridintegration.lbl.gov/der-cam.
[30] Alhamwi A, Medjroubi W, Vogt T, Agert C. Development of a GIS-based platform for the allocation and optimisation of distributed storage in urban energy systems. Appl Energy 2019;251:113360.
[31] Fonseca JA, Nguyen TA, Schlueter A, Marechal F. City Energy Analyst (CEA): integrated framework for analysis and optimization of building energy systems in neighborhoods and city districts. Energy Build 2016;113:202–26.
[32] Ruiz-Arias JA, Cebecauer T, Tovar-Pescador J, Šúri M. Spatial disaggregation of satellite-derived irradiance using a high-resolution digital elevation model. Sol Energy 2010;84(9):1644–57.
[33] Haurant P, Muselli M, Pillot B, Oberti P. Disaggregation of satellite derived irradiance maps: evaluation of the process and application to Corsica. Sol Energy 2012;86(11):3168–82.
[34] Ramirez Camargo L, Dorner W. Integrating satellite imagery-derived data and GIS-based solar radiation algorithms to map solar radiation in high temporal and spatial resolutions for the province of Salta, Argentina. In: Proceedings of Earth Resources and Environmental Remote Sensing/GIS Applications VII, 100050E; 2016 Oct 18; Edinburgh, UK. Washington, DC: Society of Photo-Optical Instrumentation Engineers (SPIE); 2016.
[35] Fu P, Rich PM. Design and implementation of the Solar Analyst: an ArcView extension for modeling solar radiation at landscape scales. In: Proceedings of the Nineteenth Annual ESRI User Conference; 1999 Jul 26–30; San Diego, CA, USA; 1999.
[36] European Commission. Photovoltaic geographical information system [Internet]. Brussels: European Commission; 2020 Mar 1 [cited 2022 Jan 12]. Available from: http://re.jrc.ec.europa.eu/pvgis/apps4/pvest.
[37] Marion B, Anderberg M, Gray-Hann P. Recent revisions to PVWATTS. In: 2005 DOE Solar Energy Technologies Program Review Meeting; 2005 Nov 7–10; Denver, CO, USA. Washington, DC: US Department of Energy Office of Scientific and Technical Information; 2005.
[38] de Sousa L, Eykamp C, Leopold U, Baume O, Braun C. iGUESS-a web based system integrating urban energy planning and assessment modelling for multi-scale spatial decision making. In: Seppelt R, Voinov AA, Lange S, Bankamp D. editors. Proceedings of the 6th International Congress on Environmental Modelling and Software; 2012 Jul 1; Leipzig, Germany. Barcelona: International Environmental Modelling and Software Society; 2012.
[39] Mohajeri N, Assouline D, Guiboud B, Bill A, Gudmundsson A, Scartezzini JL. A city-scale roof shape classification using machine learning for solar energy applications. Renew Energy 2018;121:81–93.
[40] Miyazaki H, Kuwata K, Ohira W, Guo Z, Shao X, Xu Y, et al. Development of an automated system for building detection from high-resolution satellite images. In: Proceedings of the 4th International Workshop on Earth Observation and Remote Sensing Applications (EORSA); 2016 Aug 29; Guangzhou, China. New York City: Institute of Electrical and Electronics Engineers (IEEE); 2016. p. 245–9.
[41] Dwivedi UK, Guo Z, Miyazaki H, Batran M, Shibasaki R. Development of population distribution map and automated human settlement map using high resolution remote sensing images. In: Proceedings of 2018 IEEE International Geoscience and Remote Sensing Symposium; 2018 Jul 22–27; Valencia, Spain. New York City: Institute of Electrical and Electronics Engineers (IEEE); 2018. p. 7224–7.
[42] Robinson D, Campbell N, Gaiser W, Kabel K, Le-Mouel A, Morel N, et al. SUNtool—a new modelling paradigm for simulating and optimising urban sustainability. Sol Energy 2007;81(9):1196–211.
[43] Alhamwi A, Medjroubi W, Vogt T, Agert C. GIS-based urban energy systems models and tools: introducing a model for the optimisation of flexibilisation technologies in urban areas. Appl Energy 2017;191:1–9.
[44] Pagani GA, Aiello M. From the grid to the smart grid, topologically. Phys A 2016;449:160–75.
[45] Aiello M, Fiorini L, Georgievski I. Handbook of smart energy systems. Berlin: Springer; 2021.
[46] Fowler M, Lewis J. Microservices: a definition of this new architectural term [Internet]. Chicago: Martin Fowler; 2014 Mar 25 [cited 2022 Jan 12]. Available from: https://martinfowler.com/articles/microservices.html.
[47] Newman S. Building microservices: designing fine-grained systems. Cambridge: O'Reilly Media; 2015.
[48] Bottaccioli L, Di Cataldo S, Acquaviva A, Patti E. Realistic multi-scale modeling of household electricity behaviors. IEEE Access 2019;7:2467–89.
[49] Younes S, Claywell R, Muneer T. Quality control of solar radiation data: present status and proposed new approaches. Energy 2005;30(9):1533–49.
[50] Grandjean A, Adnot J, Binet G. A review and an analysis of the residential electric load curve models. Renew Sustain Energy Rev 2012;16(9):6539–65.
[51] Torriti J. A review of time use models of residential electricity demand. Renew Sustain Energy Rev 2014;37:265–72.
[52] Istituto Nazionale di Statistica (ISTAT). Household energy consumption: public use micro.stat files. Rome: ISTAT; 2017.
[53] Lang T, Gloerfeld E, Girod B. Don't just follow the sun. A global assessment of economic performance for residential building photovoltaics. Renew Sustain Energy Rev 2015;42:932–51.
[54] Paul BM, Doyle J, Stabler B, Freedman J, Bettinardi AO. Multi-level population synthesis using entropy maximization-based simultaneous list balancing. In: Transportation Research Board 97th Annual Meeting; 2018 Jan 7–11; Washington. DC, USA. Washington, DC: National Academy of Sciences; 2018.
[55] Metropolitan Planning Organizations (MPOs). ActivitySim [Internet], San Francisco: GitHub, Inc.; 2015 [cited 2019 Sep 13]. Available from: https://activitysim.github.io/.
[56] Weather Underground [Internet]. Atlanta: The Weather Company; 2014 [cited 2022 Jan 12]. Available from: https://www.wunderground.com/.
[57] Istituto Nazionale di Statistica (ISTAT). Multipurpose survey on households-time use: public use micro.stat files. Rome: ISTAT; 2018.
[58] Reinhardt A, Baumann P, Burgstahler D, Hollick M, Chonov H, Werner M. et al. On the accuracy of appliance identification based on distributed load metering data. In: Proceedings of 2012 Sustainable Internet and ICT for Sustainability (SustainIT); 2012 Oct 4–5; Pisa, Italy. New York City: Institute of Electrical and Electronics Engineers (IEEE); 2012. p. 1–9.
[59] Bottaccioli L, Macii E, Patti E, Estebsari A, Pons E, Acquaviva A. PVInGrid: a distributed infrastructure for evaluating the integration of photovoltaic systems in smart grid. In: Camarinha-Matos L, Parreira-Rocha M, Ramezani J, editors. Proceedings of the 8th IFIPWG5.5/SOCOLNET Advanced Doctoral Conference on Computing, Electrical and Industrial Systems; 2019 May 3–5; Costa de Caparica, Portugal. Berlin: Springer; 2017. p. 316–24.
[60] Bottaccioli L, Estebsari A, Pons E, Bompard E, Macii E, Patti E, et al. A flexible distributed infrastructure for real-time cosimulations in smart grids. IEEE Trans Ind Inf 2017;13(6):3265–74.
[61] Molitor C, Gross S, Zeitz J, Monti A. MESCOS—a multienergy system cosimulator for city district energy systems. IEEE Trans Ind Inf 2014;10(4):2247–56.
[62] The European Parliament and the Council of the European Union. Directive (EU) 2018/844 of the European Parliament and of the Council of 30 May 2018 amending Directive 2010/31/EU on the energy performance of buildings and Directive 2012/27/EU on energy efficiency. Off J Eur Union 2018;L156:75–91.
[63] Commission E. Harmonised European time use surveys. Luxembourg: Eurostat; 2010.
[64] Istituto Nazionale di Statistica (ISTAT). Italian general censuses of population and housing. Rome: ISTAT; 2011.
[65] Amme J, Pleßmann G, Bühler J, Hülk L, Kötter E, Schwaegerl P. The eGo grid model: an open-source and open-data based synthetic medium-voltage grid model for distribution power supply systems. J Phys Conf Ser 2018;977:012007.
[66] Mateo Domingo C, Gomez San Roman T, Sanchez-Miralles A, Peco Gonzalez JP, Candela MA. A reference network model for large-scale distribution planning with automatic street map generation. IEEE Trans Power Syst 2011;26(1):190–7.
[67] Grzanic M, Giacomo Flammini M, Prettico G. Distribution network model platform: a first case study. Energies 2019;12(21):4079.
[68] Malya PP, Fiorini L, Rouhani M, Aiello M. Electric vehicles as distribution grid batteries: a reality check. Energy Inform 2021;4(Suppl 2):S29.